Prediction of pedestal formation in DIII-D Tokamak Plasmas using BALDUR and TASK/TR codes

Y. Pianroj[1], T. Onjun[1], A. Fukuyama[2], R. Picha[3], and N. Poolyarat[4]

[1]*School of Manufacturing Systems and Mechanical Engineering, Sirindhorn International Institute of Technology, Thammasat University, Pathum Thani,12121, Thailand*

[2]*Department of Nuclear Engineering, Kyoto University, Kyoto 606-8501, Japan.*

[3]*Thailand Institute of Nuclear Technology, Bangkok, Thailand*

[4]*Department of Physics, Thammasat University, Pathumthani, Thailand*

I. Introduction

The enhanced performance in tokamak plasmas widely known as "High confinement mode" (*H*-mode) mainly results from a formation of transport barrier at the edge of plasmas. This edge transport barrier (ETB) is usually referred as the "pedestal". Normally, the energy content in an *H*-mode discharge is approximately twice of that in a low confinement mode for similar plasmas with the same input power [1]. Theoretically, a pedestal can be formed due to a stabilization or decorrelation of micro turbulence near the plasma edge. The stabilization mechanisms, which can suppress turbulent modes, have to take into an account for the different dynamical behaviours of the various species in the plasma. The first candidate for edge turbulence stabilization is the stabilization by the $\omega_{E\times B}$ flow shear. The $\omega_{E\times B}$ flow shear can suppress turbulence by linear stabilization of turbulent modes, and in particular by non-linear decorrelation of turbulence vortices [2-4], thereby reducing transport by acting on both the amplitude of the fluctuations and the phase between them [5]. The second candidate is the magnetic shear stabilization, which is reduced only in the region where the magnetic shear exceeds its threshold. In this work, the anomalous core transport Mixed Bohm/gyro-Bohm (Mixed B/gB) model [6] is extended to describe the pedestal formation in both of integrated predictive modelling codes, BALDUR and TASK/TR. This anomalous transport is suppressed by the suppression function, which composes of both $\omega_{E\times B}$ flow shear and magnetic shear in every channel of transport coefficients.

$$f_{s_x} = \frac{1}{1 + C_x \left(\frac{\omega_{E\times B}}{\gamma_{ITG}}\right)^2} \times \frac{1}{\max\left(1, (s-0.5)^2\right)}$$

$$\chi_{i_s} = \chi_i \times f_{s_{ion}} \; ; \quad \chi_{e_s} = \chi_e \times f_{s_{electron}} ; \quad D_{H_s} = D_H \times f_{s_{Hydrogenic}} ; \quad D_{z_s} = D_z \times f_{s_{impurity}}$$

where, C_x is the optimization coefficients, γ_{ITG} is the liner ion temperature gradient (ITG) growth rate [7], s is the magnetic shear, $\chi_{i_s}$is the suppressed ion thermal diffusivity, χ_{e_s} is the suppressed electron thermal diffusivity, D_{H_s} is the suppressed hydrogenic particle diffusivity, and D_{z_s} is the suppressed impurity particle diffusivity. The values of C_x used in this work are shown in Table1.

Table 1: The optimization coefficients for each species.

Code	C_i	C_e	C_H	C_z
BALDUR	3.89×10^3	3.98×10^3	1.28×10^2	1.21×10^2
TASK/TR	1.00×10^0	1.00×10^0	-	-

Note that the value of C_x used in BALDUR code is found by optimizing an agreement of RMS between the predicted plasma profiles and corresponding experimental data; whereas the coefficients for TASK/TR is fixed at 1.0. In addition, the density profiles are predicted in the BALDUR simulations; whereas the density profiles are prescribed in the TASK/TR simulations. Lastly, the effects of ELMs are not included in all simulations in this work.

II. Simulation results

The average of RMSs, which carried out by BALDUR and TASK/TR codes, are shown in Fig.1.

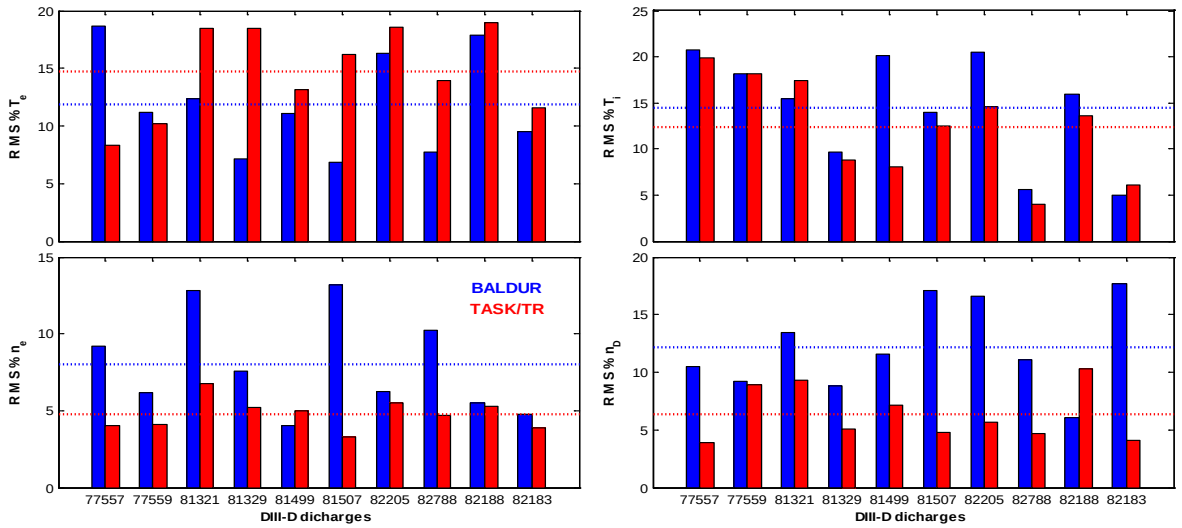

FIG.1: The RMS(%) for all profiles; electron temperature, ion temperature, electron density, and deuterium density produced by simulation using the suppression function from BALDUR and TASK/TR, compared with experimental data for 10 DIII-D *H*-mode discharges. Dash lines in each graph panel represent the average of the RMS(%).

In Fig.1, the RMS for each discharge varies from one to another. The agreement for the density tends to be better than the temperature. The average RMSs for BALDUR and TASK/TR simulations are summarized in Table2.

Table 2: Summary of the average RMS from BALDUR and TASK/TR codes.

Channel of C_x	**Average RMS**	
	BALDUR	**TASK/TR**
Electron temperature	11.87	14.78
Ion temperature	14.53	12.32
Electron density	7.99	4.78
Deuterium density	12.21	6.40

Moreover, these results are in agreement with the prediction from *L-H* power threshold (P_{L-H}) model that predicts an *L-H* transition when the heating power exceeds the power threshold. In Fig.2, it shows the P_{NBI}, P_{L-H}, $n_{e_{bar}}$, n_{e_0} and W_{tot} as a function of time for the gyro-radius (ρ^*) scan discharges (82205: low ρ^* and 82788: high ρ^*) which carried out by BALDUR. It can be seen in Fig.2 that the simulated plasmas illustrate a transition from low confinement mode to high confinement mode, indicated by an enhancement of plasma density and plasma stored energy. Both electron density (both at the center and on average) and plasma stored energy rise after the auxiliary heating is turned on. The power threshold for the transition from *L*-mode to *H*-mode is expressed in the following empirical expression [8]: $P_{L-H}[MW] = 2.84 M_{AMU}^{-1} B_T^{0.82} n_{e,20}^{-0.58} R^{1.00} a^{0.81}$, where M_{AMU} is the ion mass, B_{T} is the toroidal magnetic field, $n_{\mathrm{e,20}}$ is the electron density, R is the major radius, and a is the minor radius. This agreement for *L-H* transition between simulations and the power threshold model can be seen in all simulations for this work.

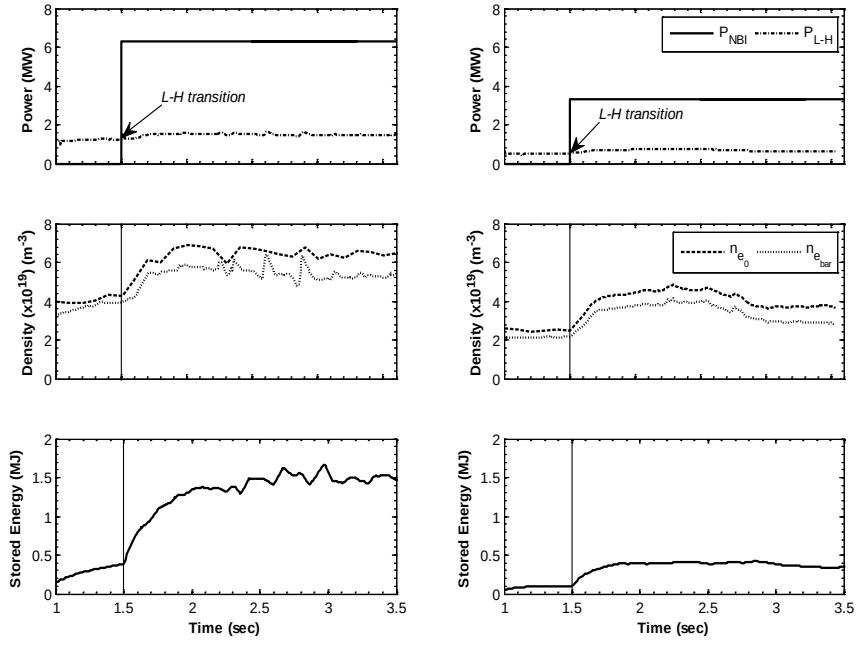

FIG.2: The NBI heating power (P_{NBI}), *L-H* transition threshold power (P_{L-H}), electrons density at the plasma core (n_{e_0}), electron line average density ($n_{e_{bar}}$) and plasma stored energy, carried out by BALDUR, as a function of time. The left panels represent the low gyro-radius scan of DIII-D discharge 82205, and the right panels represent the high gyro-radius scan of DIII-D device discharge 82788.

The capability of BALDUR and TASK/TR codes for predicting the pedestal width and pedestal height is investigated by comparing the prediction width and height to the experimental data Fig. 3 shows the pedestal width (%) of electron temperature, and the top pedestal of electron temperature between simulation results and experimental results. The correlation coefficients (R^2) of BALDUR and TASK/TR are shown in this figure. It is found that, the pedestal top of electron which carried out by TASK/TR code shows a good correlation between simulation and experiment with R^2 = 0.96. However, other parameters are not predicted well by both codes; because, the data patterns are not located on the 45 degree line.

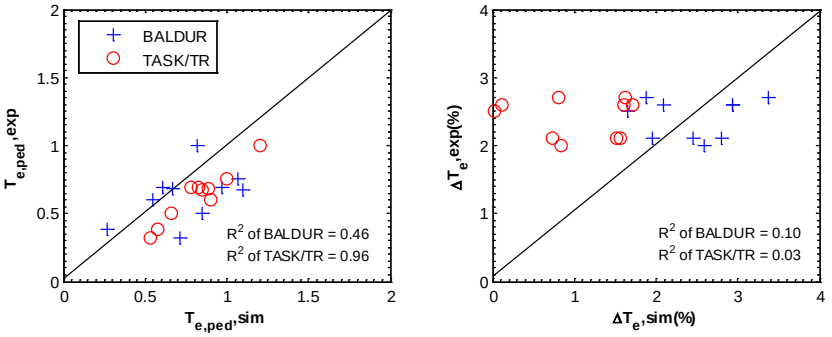

FIG.3: The electron temperature at top pedestal (left panel) and the percentage of electron temperature width (right panel), predicted by BALDUR and TASK/TR codes, compared with experimental data from 10 DIII-D *H* discharges.

III. Conclusions

A theory based pedestal transport model in which the effect of $\omega_{E\times B}$ flow shear and magnetic shear are included is developed and implemented in BALDUR and TASK/TR integrated predictive modelling codes. It is found that the simulations using both codes can reproduce experimental data. They yield the average RMS of electron temperature, ion temperature, electron density, and deuterium density less than 21% for 10 *H*-mode discharges. Furthermore, the simulations can demonstrate the *L-H* transition similar to what observed in the experiments. The predictions of pedestal width and pedestal top values using both codes are in the good range of the experimental data.

IV. Acknowledgments

This work is supported by the Commission on Higher Education (CHE), Thailand, under the program “Strategic Scholarships for Frontier Research Network for the Ph.D. Program Thai Doctoral Degree”. This work is also partially supported by a Grant-in-Aid for Scientific Research (S) (20226017) from JSPS, Japan.

References

[1] Connor J. W. and Wilson H. R. 2000 *Plasma Physics and Controlled Fusion* **42** R1-R74
[2] Biglari H. *et al* 1990 *Physics of Fluids B: Plasma Physics* **2** (1) 1-4
[3] Gohil P. 2006 *Comptes Rendus Physique* **7** (6) 606-621
[4] Boedo J. *et al* 2000 *Nuclear Fusion* **40** 1397
[5] Oost G. V. *et al* 2003 *Plasma Physics and Controlled Fusion* **45** 1-23
[6] Onjun T. and Pianroj Y. 2009 *Nuclear Fusion* **49** 075003
[7] Tala T. J. J. *et al* 2001 *Plasma Physics and Controlled Fusion* **43** 507-523
[8] Shimomura Y. *et al*, presented at the IAEA Fusion Energy Conference, Sorrento, Italy, 2000 (unpublished).